Fabrication and characterization of High Efficiency Si Solar cells using two varieties of Al paste as back surface field (BSF)

[1]Michael A. Awaah, [2]Isibhakhomen Awaah, [3]Uwadiae Obahiagbon and [4]Vitus A. Apalangya
[1]Faculty Member, CHSS Grand Canyon University, 3300 W. Camelback Road, Phoenix AZ 85017 USA
[2] Senior Process Engineer, 3320 E Yellowstone Place, Chandler Arizona 85249 USA
[3] Graduate Student, Electrical Engineering Dept., Arizona State University. Tempe, AZ, 85281 USA
[4] Lecturer, Dept. of Food Process Engineering, School of Engineering, University of Ghana, Legon, Ghana

Received: 11.15.2016/ Accepted: 11.23.2016
Abstract: Photovoltaic solar cells offer many advantages in energy generation. Aside the little maintenance requirements, they are relatively benign to the environment, generating electricity with zero greenhouse gas emission. However, a major drawback to date has been high initial cost. In order, for photovoltaics to be viable for large-scale energy conversion, their efficiency must be improved whilst making them cheaper. In this work, baseline Si Solar cells with good light conversion efficiencies was fabricated with two types of Al BSF pastes. High performance a-SiN:H was grown by PECVD. Current challenges with the Al/Ag firing process for the Sun Chemical product (CTX 0435) is detailed, it was observed that the current process disintegrates to powder substance after Ag firing; this obviates the need for process optimization. It was observed that the process window for firing the DuPont Ag front-side paste is large and yields low series resistance values without forming gas anneal (FGA anneal).

Keywords: Si Solar Cells, High Efficiency Si Solar Cell, Si solar cell using Al back surface field, Back surface field (BSF).

I. INTRODUCTION

Two major types of PV systems are available on the market today: flat plate and concentrators. As the most prevalent type of PV systems, flat plate systems builds the PV modules on a rigid and flat surface to capture sunlight. Concentrator systems use lenses to concentrate sunlight on the PV cells and increase the cell power output [1].

With single-junction single crystal solar cells now reliably approaching an efficiency of 25% [2, 3], the need for low cost processing has received a lot of attention over many decades [1]. Single junction solar cell typically consists of a junction formed between n-type and p-type semiconductors, either of the same material (homojunction) or different materials (heterojunction). Among many technologies, the major types of materials are crystalline silicon and thin films [1, 4], which vary from each other in terms of light absorption efficiency, energy conversion efficiency, manufacturing technology and cost of production. Single crystalline silicon cells are the most common in the PV industry. The main technique for producing single crystal silicon is the Czochralski (CZ) method in which high-purity polycrystalline is melted in a quartz crucible [5]. A single-crystal silicon seed is dipped into this molten mass of polycrystalline silicon. As the seed is pulled slowly from the melt, a single-crystal ingot is formed. The ingots are then sawed into thin wafers, polished, doped, coated, interconnected and assembled into modules and arrays.

A single crystal silicon has a uniform molecular structure. Compared to non-crystalline materials, its high uniformity results in higher energy conversion efficiency. The presence of deep defect states, interface and surface states, can significantly affect minority carrier lifetime [4].

In this work, prime quality p-type CZ (100) Si wafers from Si Quest were employed and processed using standard baseline Si flow. Baseline Si Solar cells with good light conversion efficiencies was fabricated and used to study the effect of two types of Al BSF pastes [6]. We also show that the process window for firing the DuPont Ag front-side paste is large and yields low series resistance values without forming gas anneal (FGA anneal) [6 – 16]

II. METHODOLOGY

Prime quality p-type CZ (100) Si wafers were employed and processed using standard baseline Si flow, with nitride film deposited by PECVD. Half the wafers (SPL-0091, 0092, 0093) were coated with Al BSF paste from Sun Chemical while the other half (SPL-0094, 0095, 0096) coated with Al paste from DuPont chemicals. At the Al firing step, three of the wafers (one coated with Sun Chemical Al paste and other two coated with DuPont Al paste) received the baseline treatment (pyro temp 826, 838, 836 ^{o}C for 30sec), while the other three were fired with a different recipe at 797, 799, 795 ^{o}C for 3 sec.
[7 – 12]. The peak firing temperature for the Ag paste was 714 ^{o}C. All six wafers had good adhesion on the front side Ag grid and back side Al after Al firing process. However, a number of wafers coated with Sun Chemical Al (CTX 0435) paste began to disintegrate after Ag firing step.
Sample SPL-0091 in figure 1, which was "accidentally" fired using the DuPont BSF recipe saw a peak temp of about 826 °C with a ~30 second ramp from 700°C. BSF completely blistered with small brown spot in normal low-right-center area. Sheet resistance measured and determined to be 147 mΩ/sq (Rs_{avg}=147.6 ± 28.0 mΩ/sq). Normal Sheet resistance data are about 10 mΩ/sq. SPL-0092 was fired with original CXT-0435 Al recipe with a peak temperature of 797°C and a ~3.8 sec ramp from 460-780°C prior to stabilizing. The wafer looked good after firing except for brown observed in normal locale. After Ag firing, bubbling and disintegration was observed everywhere except for the brown spots. Sheet resistance of 7.9 mΩ/sq (Rs_{avg} 7.9 ± 1.2 mΩ/sq) was measured.
Three of the wafers received a post process FGA (20 minutes, 400C, MRL furnace) with flash test and EL measurements taken before and after.

III. RESULTS AND DISCUSSION

Reasonable minority carrier lifetime values (µs) were measured after the POCl diffusion and after silicon nitride arc layer deposition, figure 1. The lifetime values look reasonably unchanged due to processing steps indicated.

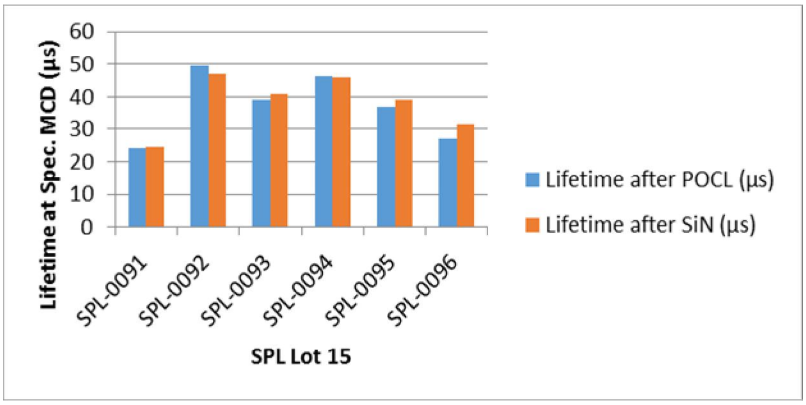

Figure 1: Lifetime measurement (MCD = 1.0x 10^{14} /cm^{3})

Figure 2 shows the optical plot of refractive index (*n*) and extinction coefficient (*K*) vs. wavelengths (λ) of light for the 78 nm amorphous hydrogenated silicon nitride (a-SiNx:H) deposited by PECVD. This data was collected from Variable Angle Spectroscope Ellipsometry (VASE) tool. The *k* values remained unchanged with an increase in *n* parameter after firing.

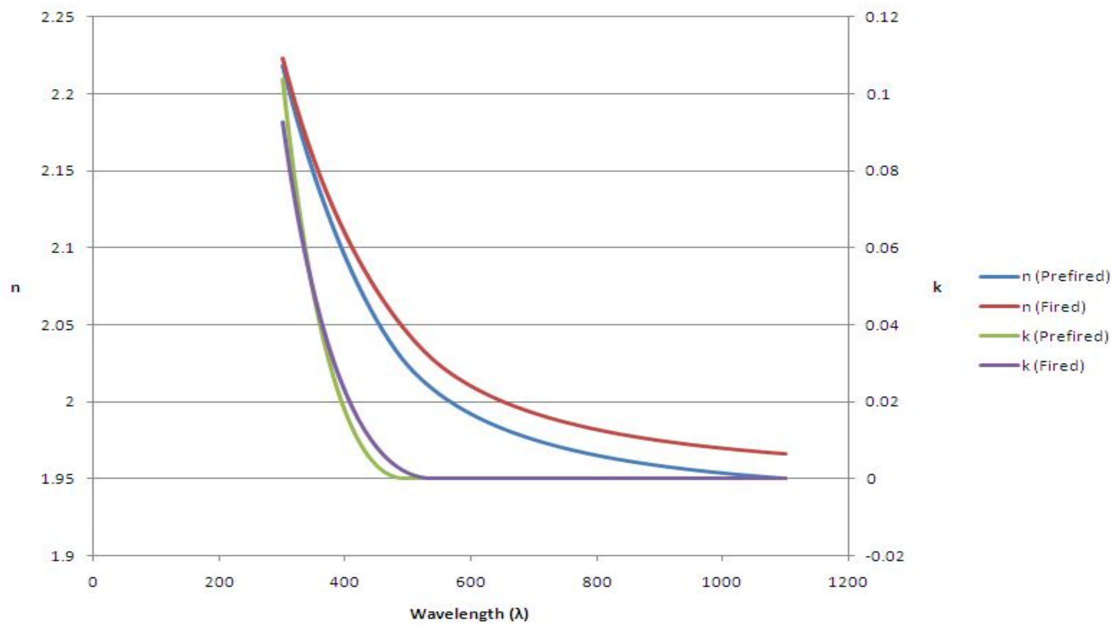

Figure 2: Plot of n, k as function of λ

Tables 1 contains RBS characterization data for PECVD deposited silicon nitride, pre- and post-firing. The target stoichiometric composition of Si:N:H after deposition was 40:42:18. After firing, N composition increased while the H composition reduced in the arc layer.

Table 1: RBS data for PECVD deposited amorphous hydrogenated SiN_x (a-SiN:H)

Sample	Si	N	H
Unfired	38.9	43.3	17.8
Fired	41.0	46.5	12.5

Few days after Ag firing, cells SPL-0092, 0093 and 0094 began to bubble and disintegrate everywhere forming a powder.
Table 2 and figures 3 and 4 contain flash test data and representative EL (electroluminescence) images for the lot. Flash tests showed reasonable solar cells conversion efficiencies ranging from 12.71 – 13.44%, low series resistance (0.55 – 0.88 Ω-cm^2), except for SPL-0091, which showed a high resistance of 1.8 Ω-cm^2, which suggests this, is not a contact resistance problem. Open circuit voltage, V**oc** of 605 mV was consistent in all the cells while an average Fill Factor (FF) of 78% was recorded.
Though several of the cells disintegrated with powdered substance everywhere, no degradation in cell performance was observed.
Three of the wafers received a post process forming gas anneal (FGA- 95% nitrogen and 5 % hydrogen) for 20 minutes at 400^{o}C in MRL furnace. The flash test data and EL images are summarized in table 3 and figures 3 & 4. After FGA treatment, the series resistance and efficiency of SPL-0091 remained unchanged.
The two other cells, SPL-0092 and 0096 with low series resistances pre-FGA treated saw an increase in series resistances and degrade efficiencies. Efficiencies in both cells dropped by 5% with increase in series resistance of 100% and 150% respectively. The reasons for this are not understood at this time.

For the SPL-0092 cell, a microscope inspection showed evidence of broken grids connected to busbar (broken fingers).

Table 2: Performance results of cells.

Wafer ID	Eff (%)	Voc (mV)	Vmp (mV)	Isc (A)	Imp (A)	FF (%)	Jsc (mA/cm^2)	Jmp (mA/cm^2)	Rsh (Ω-cm^2)	Rs (Ω-cm^2)
SPL-0091	12.84	604	482	2.92	2.67	73.7	28.9	26.6	1629	1.8
SLP-0092	13.13	605	510	2.78	2.60	78.9	27.5	25.7	2621	0.68
SPL-0093	12.71	605	526	2.77	2.44	76.6	27.4	24.2	4108	0.88
SPL-0094	12.92	604	505	2.74	2.58	78.9	27.1	25.6	3741	0.70
SPL-0095	13.25	605	506	2.23	2.09	78.5	27.9	26.2	3779	0.83
SPL-0096	13.44	605	511	2.83	2.66	79.3	28.0	26.3	2204	0.55

Table 3: Performance results of cells after FGA.

Wafer ID	Eff (%)	Voc (mV)	Vmp (mV)	Isc (A)	Imp (A)	FF (%)	Jsc (mA/cm^2)	Jmp (A/cm^2)	Rsh (Ω-cm^2)	Rs (Ω-cm^2)
SPL-0091	12.84	604	482	2.92	2.67	73.7	28.9	26.6	1629	1.8
SLP-0091 FGA	12.83	602	483	2.90	2.68	74.4	28.7	26.5	1601	1.65
SLP-0092	13.13	605	510	2.78	2.60	78.9	27.5	25.7	2621	0.68
SPL-0092 FGA	12.54	603	490	2.75	2.59	76.9	27.3	25.6	2446	1.35
SPL-0096	13.44	605	511	2.83	2.66	79.3	28.0	26.3	2204	0.55
SPL-0096	12.82	604	495	2.82	2.61	76.0	28.0	26.0	2373	1.38

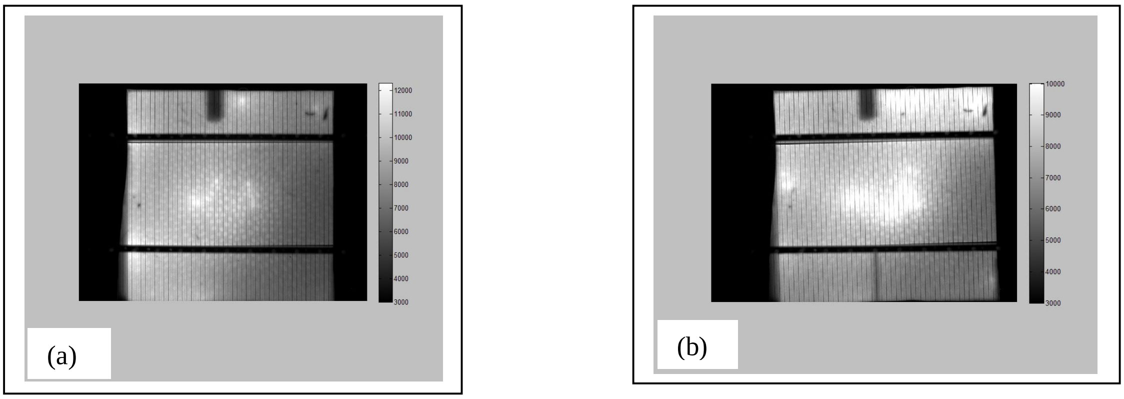

Figure 3: (a) SPL-0091 3A_1min. (b) SPL-0091 3A_1min after FGA

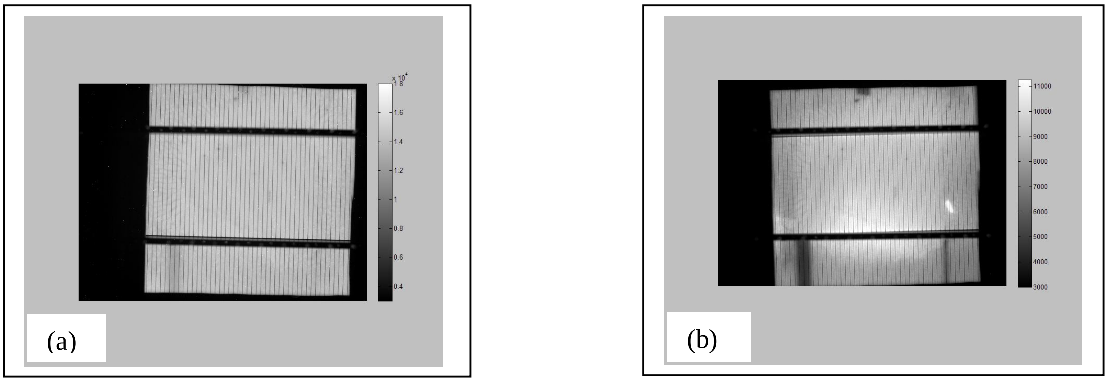

Figure 4: (a) SPL-0092 3A_1min. (b) SPL-0092 3A_1min after FGA

Quantum efficiency measurement revealed decent cells were fabricated, with EQE conversion efficiencies of above 90% in the 660 and 690 nm wavelength range.

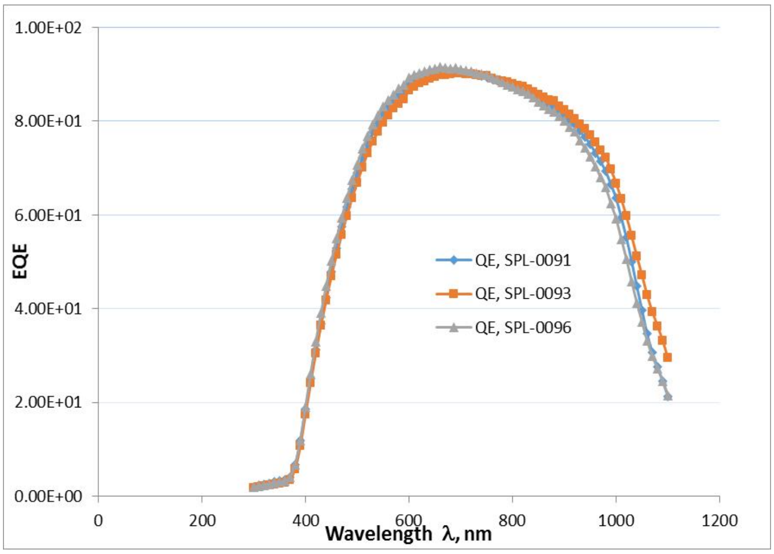

Figure 5: EQE efficiency measurement for SPL Lot15

IV. CONCLUSION

- Baseline Si Solar cells with good light conversion efficiencies was fabricated with two types of Al BSF pastes.
- The PECVD nitride performance was comparable to that obtained from other similar processes.
- The Al/Ag firing process for the Sun Chemical product (CTX 0435) needs to be optimized as the current process disintegrates to powder substance after Ag firing.
- The process window for firing the DuPont Ag front-side paste is large and yields low series resistance values without an FGA anneal.
- The quantum efficiency measurement revealed good cells.

REFERENCES

[1] A. Luque. and S. Hegedus, (eds). Handbook of Photovoltaic Science and Engineering, 2011 2nd Ed. Wiley.
[2] National Renewable Energy Lab (NREL). 2016. Latest Efficiency Records. [Online] Available at: http://www.nrel.gov/pv/assets/images/efficiency_chart.jpg [Accessed 26 November, 2016].
[3] Green, Martin A., et. al., Solar cell efficiency tables (version 48) Prog. Photovolt: Res. Appl. 2016; 24:905–913.
[4] S. S. Hegedus, W. N. Shafarman, 2004. "Thin Film Solar Cells: Device Measurements and Analysis, Prog. Photovolt: Res. Appl. 12: p 155-176.
[5] Streetman, B., Banerjee, 1999. Solid State Electronic Devices, 5th edition, Prentice Hall
[6] Hofmann, M., et. al., Recent developments in rear surface passivation at Fraunhofer ISE. Solar Energy Materials and Solar Cells, 2009. 93(6–7): p. 1074 -1078.
[7] Jens Müller, S.G., Karsten Bothe and Rolf Brendel, Optimizing the geometry of local aluminum-alloyed contacts to fully screen printed silicon solar cells, in 38th IEEE Photovoltaics Specialists Conference 2012: Austin.
[8] Sterk S., J. Knobloch, and W. Wettling, Optimization of the rear contact pattern of high-efficiency silicon solar cells with and without local back surface field. Progress in Photovoltaics: Research and Applications 1994. 2(1): p. 19-26.
[9] Rauer, M., et. al., Aluminum Alloying in Local Contact Areas on Dielectrically Passivated Rear Surfaces of Silicon Solar Cells. Electron Device Letters, IEEE, 2011. 32(7): p. 916-918.
[10] Urrejola E., et. al., Al-Si alloy formation in narrow p-type Si contact areas for rear passivated solar cells. Journal of Applied Physics 2010. 107(12): p. 124516-124516-5.
[11] Urrejola, E., et. al., Distribution of Silicon in the Aluminum Matrix for Rear Passivated Solar Cells. Energy Procedia 2011. 8(0): p.331-336.
[12] Narasinha, S. and A. Rohatgi. Optimized aluminum back surface field techniques for silicon solar cells in Photovoltaic Specialists Conference 1997 Conference Record of the Twenty-Sixth IEEE. 1997.
[13] Elias Urrejola, K.P., Heiko Plagwitz, and Gunnar Schubert, Silicon diffusion in aluminum for rear passivated solar cells Appl. Phys. Lett., 2011. 98(15): p. 3.
[14] Engelhart, P., et. al., Laser structuring for back junction silicon solar cells. Progress in Photovoltaics: Research and Applications, 2007. 15(3): p. 237-243.
[15] MERCK. Innovative Structuring Concepts for Solar Cell Production, 2012 20.9. 2012 [cited 2012 20thSeptember]; Available from: http://www.merck-performance-materials.com/en/solar_and _energy/isishape_topic_solar_and_energy/isishape_topic_solar_and_energy.html.